Journal of Innovative Technology, Vol.5, No. 1, pp. 1-8, March 2023
http://doi.org/10.29424/JIT.202303_5(1).0001

Gold Nanoparticles Modified Photoanode by Localized Surface Plasmon Resonance for Dye-Sensitized Solar Cell and Application Under Low Illumination

Hsueh-Tao Chou [1*], Chun-Yu Chu [2], Tien-Ming Wu [2], Guan-Yu Lin [2], Yao-chieh Wu [2], Zhi-Yi Yeh [2]

ABSTRACT

In this study, in order to investigate an optimal photoanode, Gold nanoparticles (AuNPs) are modified on the photoanode and are used to prepare the Dye-Sensitized solar cells (DSSCs). The result indicates that the PCEs of DSSCs with AuNPs are increased because the AuNPs increase the films absorbance of DSSCs by localized surface plasmon resonance (LSPR) effect. The light absorbance of Au-TiO_2 films with Physical method (Au-TiO_2) is increased as the concentration of AuNPs increases. The DSSCs of Au-TiO_2 films with AuNPs absorption peaks of 1.5 a.u. for 2 hours have optimal photovoltaic characteristics, where the short-circuit current density (J_{SC}) is 8.56 (mA/cm2), the open-circuit voltage (V_{OC}) is 0.73 (V), the fill factor (F.F.) is 0.59, and the photoelectric conversion efficiency (PCE) is 3.76 (%). Moreover, the PCEs of DSSCs with Au-TiO_2 1.5 a.u. films are improved from 3.76 % to 4.71% at a light intensity of 30 mW/cm^2.

Keywords: TiO_2, Doctor blade, Gold nanoparticles, Dye-Sensitized solar cell.

1. INTRODUCTION

Since the industrial revolution, global warming has been more serious caused by increased greenhouse gases from burning fossil fuels (Anik *et al.* 2023). This phenomenon leads to climate change which will transform ecosystems and environmental problems. Besides, every country increases the demand for energy. Because fossil fuels are limited, the human will face energy crisis in next 50 years (Angel *et al.* 2021). Therefore, the development of renewable energy such as wind energy, hydroelectric energy, geothermal energy, and solar energy is the main strategy to continue the civilization of humans (Li *et al.* 2019).

The DSSCs are composed of five parts, including transparent conducting oxide (TCO) substrate, photoanode, photosensitizer, electrolytes, and counter electrode. Especially, the photoanode is more important in DSSC. The research to develop the photoanode is the changes of material composition and morphology to enhance dye absorption, promote electron transport, and inject electrons from the dye excited state. And titanium oxide (TiO_2) is the most used material of photoanode (Pathakoti *et al.* 2020; Mahmoud *et al.* 2018).

In DSSCs, many researches have been reported to enhance the performance of photoanodes by increasing the photon harvesting efficiency. The metal nanoparticles are helpful in DSSCs because of the localized surface plasmon resonance (LSPR). LSPR is a phenomenon proposed from noble metal nanoparticles such as Au or Ag nanoparticles (NPs). In general, the AuNPs are usually used because it shows strong light absorption and scattering effect, and is more stable than other metal nanoparticles. The AuNPs have been used as the ideal candidate for optoelectronic devices application (Abouelela *et al.* 2021). The results of the photovoltaic characteristics of DSSCs show that the LSPR effect can enhance PCE which is attributed to the increase of JSC. The higher JSC is due to the improved light absorption of the dye in the existence of AuNPs which would have improved the dye to produce more charge carriers. In addition, the Schottky barrier at the AuNPs and TiO_2 interface makes the part of electrons from the dye straightly tunnel to the conduction band of the TiO_2 via AuNPs (Madigasekara *et al.* 2021)

In this study, gold nanoparticles are deposited onto photoanode with physical adsorption (Physical method), where AuNPs are prepared by using Turkevich method. The different absorbances of AuNPs are investigated to improve the devices performance of solar cells.

2. EXPERIMENTS

2.1 Materials

Anhydrous ethanol (Echo Chemical), TTIP (Titanium (IV) isopropoxide, Acros Organics), ACAC (2, 4-Pentandione, Alfa Aesar), TiO_2-P25 (Titanium Dioxide P25, Degussa), DI water, and Alpha-Terpineol (Acros Organics) are used in the preparation of photoanode. AuNPs solutions are mixed by Tetrachloroauric acid hydrate ($HAuCl_4 \cdot 3H_2O$, Alfa Aesar) and Sodium Citrate ($C_6H_5Na_3O_7 \cdot 2H_2O$, J.T.Baker). The dye solution is mixed with N719 powders (Ruilong Optical) and anhydrous ethanol (Echo Chemical). The electrolyte ingredients include LiI (Merck), I_2 (Aldrich), IonLic DMPII (Solaronix), and M 4-tert-butylpyridine ((Ruilong Optical). Fluorine-doped Tin Oxide (FTO) and Tin-doped Indium Oxide (ITO) are used as the substrates of working electrodes and Pt counter electrodes, respectively.

Manuscript received August 28, 2022; revised May 8, 2023; accepted May 9, 2023.

[1*] Professor (corresponding author), Department of Electronic Engineering, National Yunlin University of Science and Technology, Douliou, Yunlin, Taiwan 64002, R.O.C. (e-mail: chouht@yuntech.edu.tw)

[2] Student, Department of Electronic Engineering, National Yunlin University of Science and Technology, Douliou, Yunlin, Taiwan 64002, R.O.C.

2.2 Fabrication of AuNPs

Ps are mixed by using Turkevich method. Firstly, 15 ml of chloroauric acid ($HAuCl_4$) solution is added into 50 ml of deionized water and heated to 100 ℃. Secondly, 10 ml of sodium citrate solution is added into $HAuCl_4$ solution, and then keep stirring and heating for 10 minutes. Next, the different concentrations of AuNPs solution are diluted with DI water with absorption peaks of 0.5 a.u., 1 a.u., 1.5 a.u., 2.0 a.u., and 2.5 a.u., respectively.

2.3 Fabrication of TiO_2 photoanode

The TiO_2 compact layer solution is mixed with 1.5 ml of Titanium isopropoxide (TTIP), 0.5 ml of Acetic Acid (ACAC), and 3 ml of anhydrous ethanol, then the mixture is stirred by using an electromagnetic stirrer for 3 hours.

The TiO_2 colloid for doctor blade method is composed of 0.3 g of TiO_2 powder, 0.36 g of Alpha Terpineol, 0.25 ml of Acetic acid, and 1.8 g of GEL colloid, and then the mixture is stirred by using an electromagnetic stirrer for 24 hours.

Dye-sensitized solar cells are assembled with a sandwich structure, including photoanode, N719 dye, and counter electrode. Firstly, the Optically transparent conducting glasses (FTO) are cleaned by using acetone, ethanol, and deionized water into ultrasonic bath for 10 min, sequentially. Secondly, the compact layer with TTIP solution is spin-coated onto FTO glass at 5000 rpm for 20 s and annealed at 550 ℃ for 30 minutes. Finally, the TiO_2 colloid is deposited on compact layer by using doctor blade method and dried at 100 ℃ for 3 minutes, and then the dried films are annealed at 550 ℃ for 30 minutes.

2.4 Modification of TiO_2 photoanodes with AuNPs by using physical method

The AuNPs are prepared by using Turkevich method, and then are modified on the TiO_2 photoanode. The photoanodes are immersed into the different concentrations of AuNPs solution (with the absorption peaks of 0.5 a.u., 1 a.u., 1.5 a.u., 2.0 a.u., and 2.5 a.u.) for 2 hours. After cleaning with deionized water and drying at 100 ℃, the AuNPs-TiO_2 composite film is completed.

2.5 Assembly of DSSC device

A sandwich structure of DSSC is obtained by assembling the dye-adsorbing working electrode and Pt counter electrode. The electrolyte is injected into the cell by capillarity. Then the fabrication of DSSC devices is completed. Fig. 1 shows the schematic structure of DSSC.

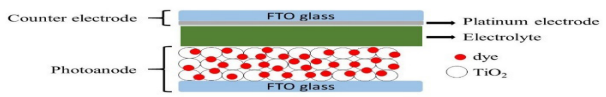

Fig. 1 The schematic structure of dye-sensitized solar cell.

2.6 Measurements and Characterization

Transmission Electron Microscopy (TEM, JEM-1400, JEOL) is used to measure the morphology of AuNPs. A field emission scanning electron microscope (FE-SEM, JSM-6701F, JEOL) is used to measure the surface morphology and thicknesses of the photoanode. An Energy Dispersive X-ray Spectroscopy (EDS) is used to observe the deposition of AuNPs. An UV-Vis spectrophotometer (V-650, JASCO) is used to measure the light absorption and dye molecules adsorption of films. A solar cell measurement system is used to measure the short circuit current density (JSC), open circuit voltage (VOC), fill factor (F.F.), and photoelectric conversion efficiency (η) of DSSCs and electrochemical impedance spectroscopy (EIS, SP-150, BioLogic) is used to provide information about the interfaces of films. The incident photon-to-current efficiency (IPCE, QE-R666, Enlitech) is used to measure the quantum efficiency of DSSCs.

3. EXPERIMENTAL

3.1 Measurements of AuNPs

In this study, AuNPs are prepared using Turkevich method, and different concentrations of AuNPs solutions are diluted with D.I. water for absorption peaks of 0.5 a.u., 1.0 a.u., 1.5 a.u., 2.0 a.u., and 2.5 a.u., respectively. The AuNPs are analyzed by using TEM as shown in Fig. 2. The smallest particle size is about 6 nm, the largest particle size is about 16 nm, and the average particle sizes of AuNPs are 10.3 nm as shown in Fig. 3. The photovoltaic characteristics of DSSCs with AuNPs modified on TiO_2 film are analyzed in the next section.

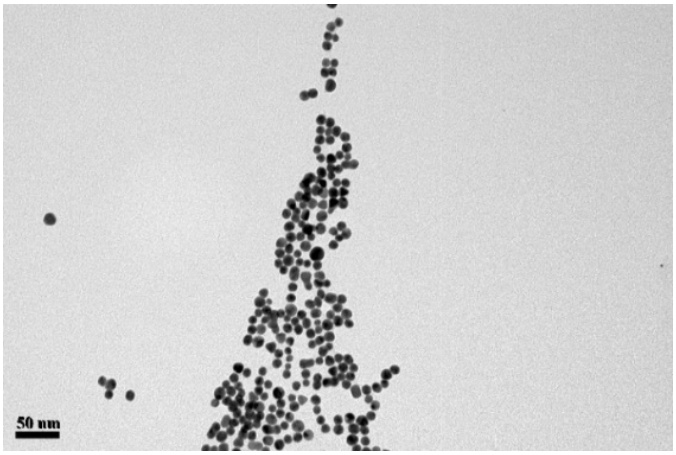

Fig. 2 TEM image of AuNPs.

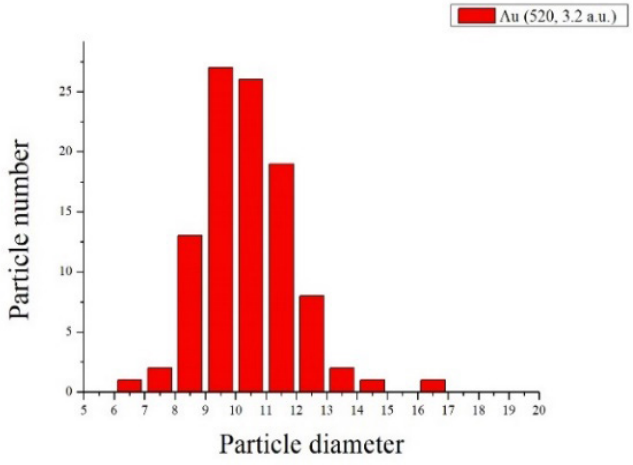

Fig. 3 The average particle sizes of AuNPs.

3.2 Thicknesses and Morphologies of Au-TiO_2 films using FE-SEM

Fig. 4 shows the FE-SEM image of cross-sectional view for TiO_2 film with 5,000 magnification. In this study, the thickness of the TiO_2 film is controlled by using doctor blade method, which is about 10 ± 1 μm. Fig. 5 (a) and (b) show the FE-SEM images for the morphology of TiO_2 film with 50000 and 100000 magnification, respectively. TiO_2 nanoparticles are uniformly deposited on the FTO surface, which is consisted of TiO_2 nanoparticles from 30 nm to 40 nm. Because the morphologies of AuNPs are similar to TiO_2 nanoparticles, and the EDX mapping images show that Ti, O, and Au elements are observed in Table 1. The Atomic percentage (Atom. C %) of photoanode with Au elements is 0.21 %, which confirms that AuNPs are successfully modified on TiO_2 film.

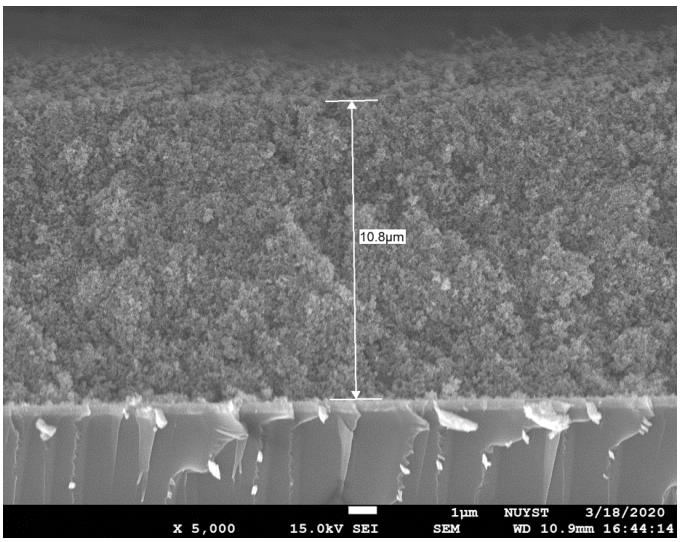

Fig. 4 Cross-sectional view of FE-SEM images of TiO_2 photoanode with 5,000 magnification.

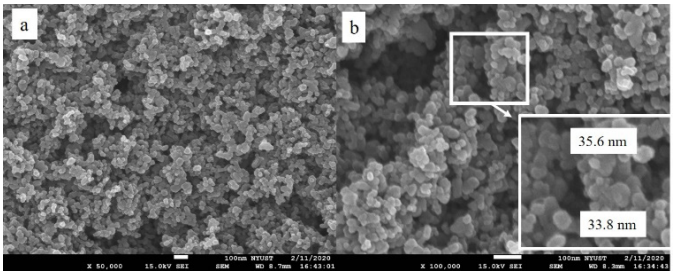

Fig. 5 FE-SEM top views of TiO_2 film with (a) 5,000 and (b) 100,000 magnification

Table 1 EDS analytical results of the DSSC with Au-TiO2 film

Element	Oxygen	Titanium	Gold
Series	K-series	K-series	M-series
Norm. C (wt %)	43.91	54.49	1.6
Atom. C (at %)	70.54	29.35	0.21
Error (wt %)	11.9	3.0	0.2

3.3 Photovoltaic characteristics of dye-sensitized solar cells

Fig. 6 (a) shows the J-V curves of DSSCs with TiO_2 film and Au-TiO_2 films, and then the photovoltaic characteristics of DSSCs are summarized in Table 2. The results show that the Au-TiO_2 films of DSSCs with AuNPs absorption peaks of 1.5 a.u. for 2 hours have highest PCE, in which JSC is 8.56 (mA/cm2), VOC is 0.73 (V), and PCE is 3.76 (%). As shown in Fig. 6 (b), compared to the pure TiO_2 photoanode, the PCEs of DSSCs with AuNPs are increased because the light absorbance of DSSCs is increased by localized surface plasmon resonance (LSPR) effect of AuNPs. The AuNPs modified on the TiO_2 photoanode can increase the local electromagnetic field and improve the light harvesting efficiency of DSSCs (Liu *et al.* 2018). The PCEs of DSSCs with AuNPs are increased because the light absorbance of DSSCs is increased due to the LSPR effect of AuNPs.

Also, it can be seen that the improvement of PCE is mainly due to the increase of the JSC, which reduces electron transfer resistance at the photoanode interface of DSSCs because of LSPR effect of AuNPs (Wang *et al.* 2021). When the Au-TiO2 films with the AuNPs absorption peaks of 2.0 a.u. and 2.5 a.u. are decreased, this result indicates that excess amounts of AuNPs on TiO_2 film will make the decrease of the dye loading.

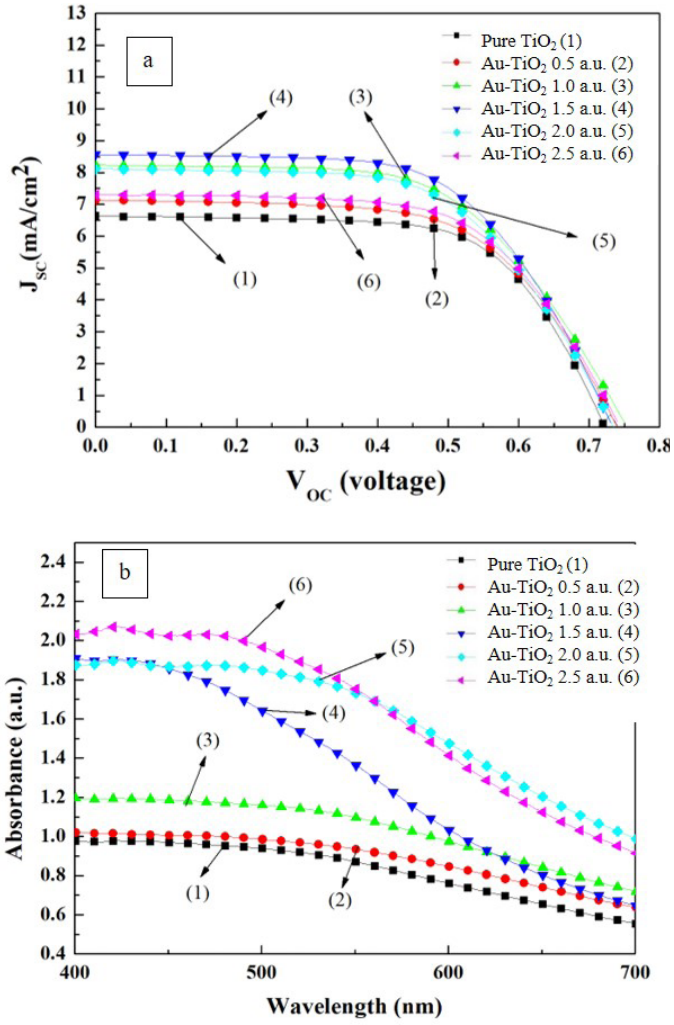

Fig. 6 (a) J-V curves and (b) Light absorbance curves of DSSCs with TiO_2 films and with Au-TiO_2 films of different concentrations of AuNPs solutions for 2 hours.

Table 2 Photovoltaic characteristics of DSSCs with TiO_2 films and Au-TiO_2 with different AuNPs solution concentrations for a deposition time of 2 hours.

Sample	J_{SC} (mA/cm^2)	V_{OC} (V)	F.F.	η (%)
Pure TiO_2	6.64	0.72	0.64	3.11
Au-TiO_2 0.5 a.u.	7.13	0.74	0.60	3.22
Au-TiO_2 1.0 a.u.	8.23	0.75	0.58	3.61
Au-TiO_2 1.5 a.u	8.56	0.73	0.59	3.76
Au-TiO_2 2.0 a.u	7.94	0.73	0.59	3.52
Au-TiO_2 2.5 a.u	7.29	0.74	0.61	3.33

3.4 Light absorbance of Au-TiO_2 film

Fig. 6 (b) shows the light absorbance of DSSCs which is modified with the different concentrations of AuNPs solutions of the TiO_2 photoanode for 2 hours, where the wavelengths are from 400 nm to 700 nm. Compared to the pure TiO_2 photoanode, the light absorbance of the Au-TiO_2 films is enhanced as the concentration of AuNPs solutions increases. The Au-TiO_2 films with AuNPs absorption peaks of 2.5 a.u. for 2 hours have the highest film light absorbance. The light absorbance of photoanode increases with the increasing deposition time of Au nanoparticles in the visible range (400~700nm), which can be attributed to LSPR effect of AuNPs to improve the interaction between electromagnetic field and TiO_2 to absorb more photons (Li *et al.* 2019; Cheng *et al.* 2006).

3.5 Dye loading of Au-TiO_2 film of different AuNPs concentrations

Fig. 7 shows the dye loading of the DSSCs with pure TiO_2 films and Au-TiO_2 films of different concentrations of AuNPs solutions for 2 hours, in which there are two characteristic peaks located at 368 nm and 495 nm.

photoanode films for the wavelength at 386.5 nm in the UV-Visible absorption spectrum. The dye concentration can be calculated from Equation 4-1.

$$A=\varepsilon*b*c \qquad \text{(Equation 4-1)}$$

, where A is absorbance, ε is molar adsorption coefficient ($M^{-1}cm^{-1}$), b is length of the path traversed by the light (cm), and c is concentration of the solution (M).

The DSSCs with pure TiO_2 films have the highest light absorbance of dye, in which the dye concentration is 27 μM. However, the light absorbance of dye with the Au-TiO_2 films has decreased as the concentration of AuNPs solution increases, and the Au-TiO_2 films with AuNPs absorption peaks of 2.5 a.u. for 2 hours have the lowest light absorbance of dye where the dye concentration is 16 μM.

The results show that the dye loading of Au-TiO_2 film with different AuNPs concentrations for 2 hours decreases due to the specific surface area of TiO_2 nanoparticles is reduced and dye loading of Au-TiO_2 film is affected (Gao *et al.* 2021).

As stated above, the performance of Au-TiO_2 films has influenced each other between the LSPR effect of AuNPs and the dye.

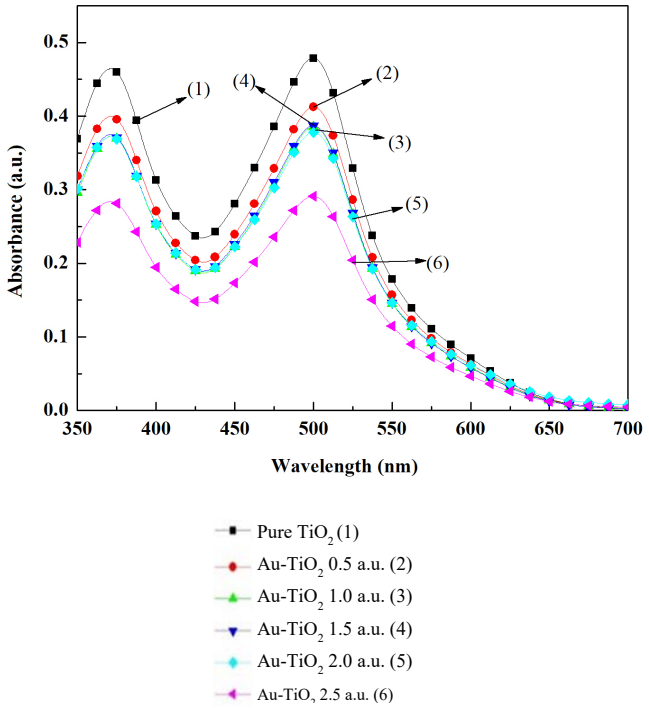

Fig. 7 Light absorbance curves of dye for the DSSCs with pure TiO_2 films and Au-TiO_2 films of different concentrations of AuNPs solutions for 2 hours.

Table 3 Dye concentration of pure TiO_2 films and Au-TiO2 films in different concentrations of AuNPs for 2 hours

Sample	Dye adsorption (a.u.)	Dye concentration (μM)
Pure TiO_2	0.401	27
Au-TiO_2 0.5 a.u.	0.346	24
Au-TiO_2 1.0 a.u.	0.333	23
Au-TiO_2 1.5 a.u	0.324	22
Au-TiO_2 2.0 a.u	0.322	21
Au-TiO_2 2.5 a.u.	0.247	16

3.6 Electrochemical properties analysis of DSSCs with Au-TiO_2 film of different AuNPs concentrations

Fig. 8 shows the Nyquist plot of DSSCs with pure TiO_2 films and with Au-TiO_2 films of different concentrations of AuNPs solutions for 2 hours. In the EIS Nyquist spectra, there are two semicircles of DSSCs. According to the EIS model for DSSC devices, the first smaller circle is the R_{ct1} which is the resistance between the electrolyte and Pt counter electrode, and the second larger circle, R_{ct2}, is the charge transfer resistance at the interface of TiO_2/dye/electrolyte (Li *et al.* 2019). The Au-TiO_2 films of DSSCs with AuNPs absorption peaks of 0.5 a.u., 1.0 a.u., 1.5 a.u., 2.0 a.u., and 2.5 a.u. are denoted as Au-TiO_2 0.5 a.u, 1.0 a.u., 1.5 a.u., 2.0 a.u., and 2.5 a.u., respectively.

As shown in Fig. 8 and Table 4, the R_{ct2}'s of DSSCs with Au-TiO_2 0.5 a.u., 1.0 a.u., and 1.5 a.u. films are respectively 9.4 Ω, 8.7 Ω, and 7.1 Ω, which are lower than the DSSCs of TiO_2 film. According to the literature, the change of R_{ct2} can be attributed

to the content of AuNPs in the TiO_2 photoanode, and the values of R_{ct2} are decreased with the increasing concentration of AuNPs, where the DSSC with Au-TiO_2 1.5 a.u. films has the lowest R_{ct2} with a value of 7.1 Ω. Moreover, the Schottky barrier is formed at the Au-TiO_2 interface. The Schottky barrier makes it easy for the electrons in the dye to be injected into conduction band of TiO_2 through the AuNPs, which can efficiently reduce the electron-hole pair recombination, thus accelerates electron injection (Ali *et al.* 2019). Therefore, the R_{ct2}'s of DSSCs with Au-TiO_2 films are lower than pure TiO_2 films.

Table 4 EIS parameters of DSSCs with pure TiO_2 films and with Au-TiO_2 films

Sample	R_S(Ω)	R_{ct1}(Ω)	R_{ct2}(Ω)	Lifetime (ms)
Pure TiO_2	12.73	1.17	9.57	11.75
Au-TiO_2 0.5 a.u.	11.26	1.03	9.4	11.75
Au-TiO_2 1.0 a.u.	12.30	1.02	8.7	14.21
Au-TiO_2 1.5 a.u	12.74	0.87	7.1	16.58
Au-TiO_2 2.0 a.u	12.93	1.64	8.02	14.44

The electron lifetime (τ_e) formula can be calculated as:

$$\tau_e = \frac{1}{2\pi f_{max}} = \frac{1}{\omega_{max}} \quad \text{(Equation 4-2)}$$

, in which τ_e is the electron lifetime, and f_{max} is the maximum frequency of the central impendence at the interface of TiO_2 /dye/ electrolyte.

The highest electron lifetime of 16.58 ms indicates that the DSSCs with Au-TiO_2 1.5 a.u. films have the lowest recombination rate and fastest electron transfer due to the LSPR effect of AuNPs. This result can help to improve the photogenerated electrons and lead to higher PCE and J_{SC}. However, the electron lifetime of DSSCs with Au-TiO_2 2.0 a.u. and Au-TiO_2 2.5 a.u. films are decreased to 14.44 ms and 12.06 ms as the AuNPs concentrations are increased. This may be attributed to that the contact of excess AuNPs with the electrolyte could increase charge recombination and cause the decrease of the J_{SC} (Hwang *et al.* 2019).

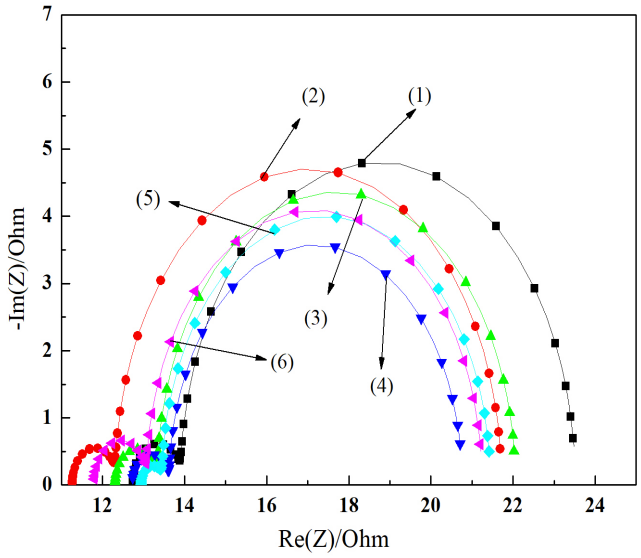

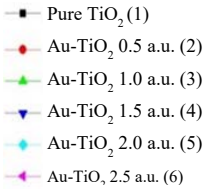

Fig. 8 Nyquist plots of DSSCs with pure TiO_2 films and with Au-TiO_2 films of different concentrations of AuNPs solutions for 2 hours.

In summary, it can be seen that the charge transfer resistance of DSSCs with Au-TiO_2 films is reduced (lower value of R_{ct2}) as the concentration of AuNPs increases, while the light absorbance also increases due to the LSPR effect, which improves the PCE and J_{SC}. The DSSCs of Au-TiO_2 1.5 a.u. films have an optimal PCE of 3.76 %.

However, the excess of AuNPs not only affects the TiO_2 nanoparticles to absorb dye molecules (the lower dye loading of photoanode) but also increases charge recombination (the bigger value of R_{ct2}) and thus decreases the PCE. This result shows that appropriate amounts of AuNPs can effectively enhance the light absorption in DSSCs photoanodes and then increase PCE of DSSCs.

3.7 IPCE analysis of DSSCs with Au-TiO_2 film of different AuNPs concentrations

Fig. 9 shows the IPCE curve of DSSCs with pure TiO_2 and with Au-TiO_2 films of different concentrations of AuNPs solutions for 2 hours. And the absorption bands of the N719 dye occur at 330 nm and 533 nm. It is observed that the DSSCs with Au-TiO_2 1.5 a.u. films have the highest quantum efficiency. IPCE curves which match with light absorbance of DSSCs with Au-TiO_2 films further verify the trend of Jsc. In the photovoltaic characteristics, the J_{SC} of DSSCs with Au-TiO_2 films is increased when the AuNPs concentration increases. This enhancement will be reflected in the IPCE, which confirmed that the photo-current generation efficiency is improved by AuNPs. The AuNPs attachment on the TiO_2 films can enhance light absorbance (local field enhancement) and charge separation (Yang *et al.* 2021). Meanwhile, the R_{ct2}'s of Au-TiO_2 films is decreased as the increase of AuNPs content in EIS measurement, which proves that the increase of AuNPs content can effectively reduce the charge transfer resistance, and both of these factors can enhance the J_{SC} of the DSSCs.

However, the quantum efficiency of DSSCs with Au-TiO_2 2.0 a.u. films and Au-TiO_2 2.5 a.u. films are decreased due to the excess of AuNPs concentration and also reflected in the IPCE quantum efficiency. These results show that only optimized concentrations can improve the performance of DSSCs.

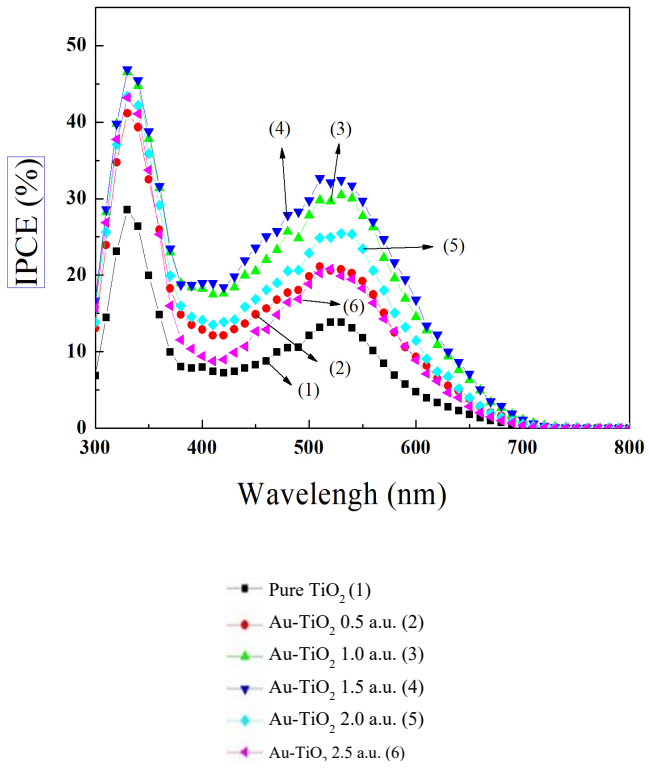

Fig. 9 IPCE curves of DSSCs with pure TiO_2 films and Au-TiO_2 films of different concentrations of AuNPs solutions for 2 hours.

3.8 Photovoltaic characteristics of DSSCs under different light intensities.

The optimal DSSCs with pure TiO_2 films and Au-TiO_2 1.5 a.u. films are chosen for the photovoltaic measurements, where the different intensities of incident light are controlled by the filter with different transmittances as shown in Fig. 10 and Table 5. The J_{SC} of DSSCs with Au-TiO_2 1.5 a.u. films is decreased from 9.97 to 0.98 mA/cm^2 when the light intensity is decreased from 100 to 10 mW/cm^2. And the V_{OC} of DSSCs with Au-TiO_2 1.5 a.u. films are decreased from 0.79 to 0.64 as the light intensity is decreased from 100 to 10 mW/cm^2. This is because of the decrease in the light intensity, resulting in the decrease of photoelectrons generated at the TiO_2/electrolyte interface (Aftabuzzaman *et al.* 2021). The F.F. of DSSCs with Au-TiO_2 1.5 a.u. films is enhanced from 0.57 to 0.71 as the light intensity is decreased from 100 to 10 mW/cm^2. The overall PCE of DSSCs with TiO_2 film is improved at low illuminance due to the electron recombination of DSSCs being decreased. But under the light intensity at 50 and 10 mW/cm^2, the PCEs of DSSCs with Au-TiO_2 1.5 a.u. films are reduced to 4.13 % and 3.77 %. According to J. L Lan's research, the PCEs of DSSCs are changed at different low light intensities which depend on the iodine content in the electrolyte, resulting in the lower ion diffusion in the electrolyte under the light intensities at 50 and 10 mW/cm^2. The reduced number of photoelectrons generated within the DSSC leads to a lower PEC (Lan *et al.* 2012; Saeed *et al.* 2021).

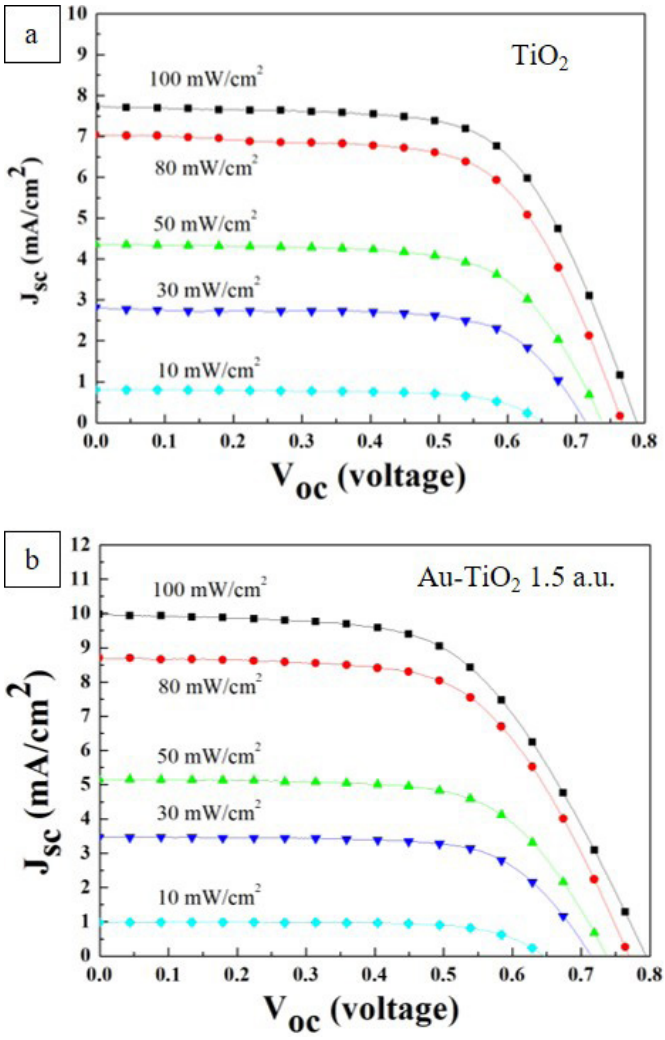

Fig. 10 J-V curves of DSSCs under different light intensities with (a) pure TiO_2 films and (b) Au-TiO_2 1.5 a.u. films.

Compared to DSSCs with pure TiO_2 films, the DSSCs of Au-TiO_2 1.5 a.u. films have higher J_{SC}. These results indicate that the LSPR effect of AuNPs also works at low light intensity, enabling the performance enhancement of DSSCs to have higher PCE. The optimal PCEs of DSSCs with Au-TiO_2 1.5 a.u. films are improved from 3.76 % to 4.71% at a light intensity of 30 mW/cm^2.

Table 5 Photovoltaic characteristics of DSSCs under different light intensities.

Pure TiO_2				
Light intensities (mW/cm^2)	J_{SC} (mA/cm^2)	V_{OC} (V)	F.F.	η (%)
100	7.73	0.78	0.64	3.29
80	7.05	0.77	0.64	3.62
50	4.36	0.73	0.66	3.56
30	2.81	0.71	0.67	3.78
10	0.8	0.64	0.68	2.95

Au-TiO_2				
Light intensities (mW/cm^2)	J_{SC} (mA/cm^2)	V_{OC} (V)	F.F.	η (%)
100	9.97	0.79	0.57	3.78
80	8.69	0.76	0.61	4.24
50	5.16	0.73	0.65	4.13
30	3.47	0.71	0.68	4.71
10	0.98	0.64	0.71	3.77

4. CONCLUSION

The AuNPs are successfully modified on TiO_2 film by using the physical method. The PCEs of DSSCs with Au-TiO_2 films are increased due to the LSPR effect of AuNPs. Moreover, the EIS measurement shows that the DSSCs with Au-TiO_2 films can reduce the recombination effect and enhance the electron transfer rate due to the LSPR effect of AuNPs. However, the excess of AuNPs not only affects the TiO_2 nanoparticles to adsorb dye molecules but also increases charge recombination and thus decreases the PCE of DSSCs. The DSSCs with Au-TiO_2 films for AuNPs absorption peaks of 1.5 a.u. for 2 hours have optimal photovoltaic characteristics, where J_{SC} is 8.56 (mA/cm^2), V_{OC} is 0.73 (V), and PCE is 3.76 (%), moreover, the LSPR effect of AuNPs works also at the low light intensity, and the PCEs of DSSCs with Au-TiO_2 films are improved from 3.76 % to 4.71% at a light intensity of 30 mW/cm^2.

REFERENCES

Abouelela, M.M., Kawamura, G., and Matsuda, A. (2021). "A review on plasmonic nanoparticle-semiconductor photocatalysts for water splitting." Journal of Cleaner Production, **290**(2), 1–17. doi.org/10.1016/j.jclepro.2021.126200

Aftabuzzaman, M., Sarker, S., Lu, C., and Kim, H.K. (2021). "In-depth understanding of the energy loss and efficiency limit of dye-sensitized solar cells under outdoor and indoor conditions." Journal of Materials Chemistry A, (44), 24830–24848. doi.org/10.1039/D1TA03309C

Ali, A.K., Erten-Ela, S., Hassoon, K.I., and Ela, Ç. (2019). "Plasmonic enhancement as selective scattering of gold nanoparticles based dye sensitized solar cells." Thin Solid Films, **671**(1), 127–132. doi.org/10.1016/j.tsf.2018.12.033

Angle, F., Shanmuga, S.P., S.Harish, K., Sudhakar, K., and Muhammad, T. (2021). "A review on recent developments in solar photoreactors for carbon dioxide conversion to fuels." Journal of CO_2 Utilization, **47**(1), 101515–101534. doi.org/10.1016/j.jcou.2021.101515

Anik, S., Miftahussurur, H.P., Abul, K.B., Anil, K.B., and Axel, G. (2023). "Insight on the choice of sensitizers/dyes for dye sensitized solar cells: A review." Dyes and Pigments, **213**(111087), 1–35. doi.org/10.1016/j.dyepig.2023.111087

Cheng, X., Chen, M., Wu, L., and Gu, G. (2006). "Novel and facile method for the preparation of monodispersed titania hollow spheres." Langmuir, **22**(8), 3858–3863. doi.org/10.1021/la0534221

Gao, Q., Zhang, X., Duan, L., Li, X., and Lü, W. (2019). "Au nanoparticle-decorated TiO_2 nanorod array for plasmon-enhanced quantum dot sensitized solar cells." Superlattices and Microstructures, 129, 185–192. doi.org/10.1016/j.spmi.2019.03.028

Ge, Z., Wang, C., Chen, Z., Wang, T., Shi, R., Yu, S., and Liu, J. (2021). "Investigation of the TiO_2 nanoparticles aggregation with high light harvesting for high-efficiency dye-sensitized solar cells." Materials Research Bulletin, **135**, 1–8. doi.org/10.1016/j.materresbull.2020.111148

Hwang, H.J., Joo, S.J., Patil, S.A., and Kim, H.S. (2017). "Efficiency enhancement in dye-sensitized solar cells using the shape/size-dependent plasmonic nanocomposite photoanodes incorporating silver nanoplates." Nanoscale, **9**(26), 7960–7969. doi.org/10.1039/C7NR01059A

Li, G., Sheng, L., Li, T., Hu, J., Li, P., and Wang, K. (2019). "Engineering flexible dye-sensitized solar cells for portable electronics." Solar Energy, **177**(1), 80–98. doi.org/10.1016/j.solener.2018.11.017

Li, M., Yuan, N., Tang, Y., Pei, L., Zhu, Y., Liu, J., Bai, L., and Li, M. (2019). "Performance optimization of dye-sensitized solar cells by gradient-ascent architecture of SiO_2@Au@TiO_2 microspheres embedded with Au nanoparticles." Journal of Materials Science & Technology, **35**(4), 604–609. doi.org/10.1016/j.jmst.2018.09.030

Lin, J.L., Wei, T.C., Feng, S.P., Wan, C.C., and Cao, G. (2012) "Effects of Iodine Content in the Electrolyte on the Charge Transfer and Power Conversion Efficiency of Dye-Sensitized Solar Cells under Low Light Intensities." The Journal of Physical Chemistry C, **116**(49), 25727–25733. doi.org/10.1021/jp309872n

Liu, C.C., Liang, M.S., and Khaw, C.C. (2018). "Effect of gold nanoparticles on the performances of TiO_2 dye-sensitised solar cell." Ceramics International, **44**(6), 5926–5931. doi.org/10.1016/j.ceramint.2017.12.158

Mahmoud, M.S., Akhtar, M.S., Mohamed, I.M.A., Hamdan, R., Dakka.Y.A. and Barakat, N.A.M. (2018). "Demonstrated photons to electron activity of S-doped TiO_2 nanofibers as photoanode in the DSSC." Materials Letters, **225**(1), 77–81. doi.org/10.1016/j.matlet.2018.04.108

Pathakoti, K., Manubolu, M., and Hwang, H.M. (2020). "Mechanistic insights into TiO_2 and ZnO nanoparticle-induced metabolic changes in Escherichia coli under solar simulated light irradiation." Water, Air, & Soil Pollution, **201**(16), 1–9. doi.org/10.1007/s11270-019-4388-2

Saeed, M.A., Yoo, K., Kang, H.C., Shim, J.W., and Lee, J.J. (2021). "Recent developments in dye-sensitized photovoltaic cells under ambient illumination." Dyes and Pigments, 194, 1–16. doi.org/10.1016/j.dyepig.2021.109626

Yang, H.Y., Lee, S.H., Kim, H.M., Pham, X.H., Hahm, E., Kang, E.J., Kim, T.H. Ha, Y., Jun, B.H., and Rho, W.Y. (2019). "Plasmonic and charging effects in dye-sensitized solar cells with Au nanoparticles incorporated into the channels of freestanding TiO_2 nanotube arrays by an electrodeposition method." Journal of Industrial and Engineering Chemistry, **80**(1), 311–317. doi.org/10.1016/j.jiec.2019.08.009

Yumei, H., Maryam, K., Anshuman, S., James, B.S., and Mohammad, A.H. (2023). "Converging concepts of sustainability and supply

chain networks: a systematic literature review approach." Environmental Science and Pollution Research **30**(1), 46120–46130. doi.org/10.1007/s11356-023-25412-y